Medicinal Chemistry

International Edition: DOI: 10.1002/anie.201701905
German Edition: DOI: 10.1002/ange.201701905

Small-Molecule Inhibition of the UNC119–Cargo Interaction

*Tom Mejuch, Guillaume Garivet, Walter Hofer, Nadine Kaiser, Eyad K. Fansa, Christiane Ehrt, Oliver Koch, Matthias Baumann, Slava Ziegler, Alfred Wittinghofer, and Herbert Waldmann**

Abstract: *N-Terminal myristoylation facilitates membrane binding and activity of proteins, in particular of Src family kinases, but the underlying mechanisms are only beginning to be understood. The chaperones UNC119A/B regulate the cellular distribution and signaling of N-myristoylated proteins. Selective small-molecule modulators of the UNC119–cargo interaction would be invaluable tools, but have not been reported yet. We herein report the development of the first UNC119–cargo interaction inhibitor, squarunkin A. Squarunkin A selectively inhibits the binding of a myristoylated peptide representing the N-terminus of Src kinase to UNC119A with an IC_{50} value of 10 nM. It binds to UNC119 proteins in cell lysate and interferes with the activation of Src kinase. Our results demonstrate that small-molecule inhibition of the UNC119–cargo interaction might provide new opportunities for modulating the activity of Src kinases that are independent of direct inhibition of the enzymatic kinase activity.*

The UNC119A and UNC119B proteins are homologous molecular chaperones that specifically bind the lipidated N-termini of N-myristoylated proteins and modulate their cellular shuttling, subcellular localization, and activity.[1] UNC119 cargo includes ciliary proteins such as nephrocystin-3[2] and N-acylated G protein α-subunits,[3] and UNC119 was linked to the trafficking and activation of the N-myristoylated Src family tyrosine kinases Lck, Lyn, and Fyn.[4] In particular, Bastiaens[5] and co-workers very recently demonstrated that UNC119 also regulates the subcellular localization and activity of the Src kinase itself, a major oncogene and target in anticancer drug discovery.[6]

[*] Dr. T. Mejuch, G. Garivet, W. Hofer, N. Kaiser, Dr. S. Ziegler, Prof. Dr. H. Waldmann
Department of Chemical Biology
Max-Planck-Institute of Molecular Physiology
Otto-Hahn-Strasse 11, 44227 Dortmund (Germany)
E-mail: herbert.waldmann@mpi-dortmund.mpg.de
Dr. T. Mejuch, G. Garivet, W. Hofer, N. Kaiser, C. Ehrt, Dr. O. Koch, Prof. Dr. H. Waldmann
Faculty of Chemistry and Chemical Biology
TU Dortmund University
Otto-Hahn-Strasse 6, 44227 Dortmund (Germany)
Dr. E. K. Fansa, Prof. Dr. A. Wittinghofer
Department of Structural Biology
Max-Planck-Institute of Molecular Physiology
Otto-Hahn-Strasse 11, 44227 Dortmund (Germany)
Dr. M. Baumann
Lead Discovery Center GmbH
Otto-Hahn-Strasse 15, 44227 Dortmund (Germany)
Supporting information and the ORCID identification number(s) for the author(s) of this article can be found under: https://doi.org/10.1002/anie.201701905.

N-Terminal protein myristoylation facilitates the reversible binding of proteins to membranes,[7] but the mechanisms dictating selective subcellular localization are only beginning to be understood. In an analogous system concerning the localization of lipidated proteins, the intermembrane shuttling, subcellular localization, and activity of C-terminally S-farnesylated proteins such as the Ras and Rheb GTP-binding proteins are mediated by the PDE6δ chaperone, which binds the lipidated C-terminus.[8] Small-molecule inhibitors of the PDE6δ–Ras and PDE6δ–Rheb interactions have proven to be invaluable tools in the unraveling of the corresponding mechanisms.[9] Moreover, the inhibition of these interactions with small molecules impairs the localization and oncogenic signaling of Ras and Rheb proteins.[10] By analogy, selective inhibitors of the interactions between UNC119 chaperones and their N-myristoylated cargo might be powerful tools for uncovering the biological mechanisms guiding the subcellular localization of the cargo proteins and might open up novel opportunities to interfere with their activity. This could be particularly relevant for the Src kinase. Src is involved in many critical processes such as cell growth, proliferation, angiogenesis, and survival.[11] Uncontrolled overexpression and overactivation of Src is observed in various cancer types,[12] and kinase inhibitors targeting the ATP-binding site of Src are in high demand.[13] However, owing to the high sequence and structural homology of kinase ATP-binding sites, such inhibitors need to be highly selective, which complicates their development.[14] Therefore, novel approaches to modulate kinase activity by alternative strategies are needed.[15]

Analysis of the crystal structure of UNC119A in complex with a myristoylated peptide[3c] using DogSite Scorer[16] to predict druggability suggests that the lipid-binding pocket of UNC119 should be amenable to targeting with small molecules (Figure 1). However, small-molecule inhibitors blocking the interaction of UNC119 with its cargo have not been identified yet.

Herein, we report the development of the first small-molecule ligand of the UNC119 lipid-binding site, named squarunkin A. Squarunkin A inhibits the binding to UNC119A of a myristoylated peptide representing the N-terminus of Src with an IC_{50} value of 10 nM and does not target the lipoprotein-binding sites of other lipoprotein chaperones, such as PDE6δ, AIPL1, and RhoGDI, which bind S-prenylated proteins. The compound binds to UNC119 in cell lysate and interferes with Src activation.

To identify small-molecule ligands for the UNC119 lipid binding site, we employed a screening assay based on the homogeneous time resolved fluorescence (HTRF) technique.[17] In the assay, GST-tagged UNC119A protein together with an anti-GST antibody fused to a Eu^{3+} cryptate

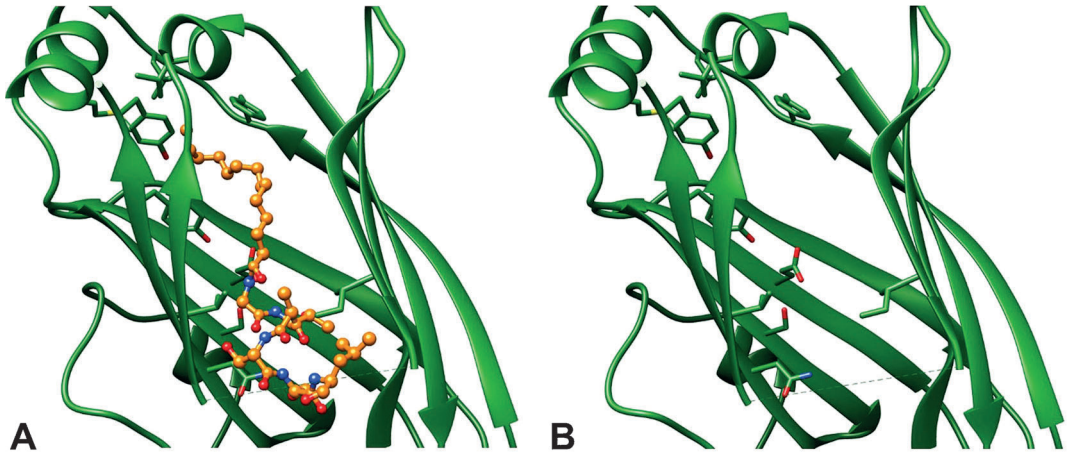

Figure 1. A) Structure of the lipid-binding protein UNC119A (green) in complex with a myristoylated NPHP3 peptide (orange sticks, PDB: 5L7K).[3c] B) The UNC119A cavity can potentially accommodate small-molecule inhibitors.

complex was used as the FRET donor. A myristoylated and biotinylated N-terminal peptide derived from the Src protein that binds to UNC119A with a K_D of 91 nM[18] and streptavidin-d2 complex served as the FRET acceptor. In the presence of an inhibitor, the complex between the donor and the acceptor is destabilized, and the emission signal from the acceptor is abolished (for an illustration of the assay principle, see Figure S1 in the Supporting Information).

Initially, our in-house compound library (ca. 200000 members) was screened to identify compounds that reduced the signal to less than 50% at 1.25 μM concentration. For the 500 most potent compounds, IC_{50} values were determined by means of the HTRF assay. Several of the most potent compounds were based on a squaramide scaffold.

Variation of the squaramide substituents (Table 1; for details, see Table S1) revealed that for activity, one substituent should be a 4-amino-substituted piperidine carrying a carbamate group. Compounds with piperazine, morpholine, or phenyl moieties instead of the 4-aminopiperidine were inactive. Moreover, whereas the N-ethoxycarbonyl-substituted inhibitor **3a** is very potent, the shorter *N*-acetyl analogue, the non-acylated aminopiperidine, and the 4-aminopyridine derivative do not inhibit the interaction (**3b**–**3d**). For the second amide substituent, the best inhibitors contained a 4-aryl-substituted piperazine attached to the squaramide core via a short alkyl linker. Replacement of the aryl group by a benzyl or alkyl group resulted in reduced or no inhibitory activity (Table S1). For the linker, two or three methylene groups are best (**3a**, **3f**, and **3g**), and in the absence of a linker, the activity is lost (**3e**). Substitution in the *meta* position of the aromatic ring yielded compounds that are more active than the corresponding *ortho*- or *para*-substituted analogues (**3a**, **3h**, and **3i**). The best results were obtained with Cl- and CF_3-substituted arenes (**3a**, **3f**, **3j**, and **3k**). Several compounds displayed low nanomolar IC_{50} values (**3a**, **3f**, **3j**, and **3k**). To prioritize the hits, we determined their kinetic solubility and investigated them in parallel artificial membrane assay (PAMPA) experiments (Table 1). The data revealed that the hits have comparable kinetic solubility (except for **3f**, which has significantly higher solubility). For compounds **3a** and **3j**, comparable membrane permeability was measured that was significantly higher than the permeability recorded for **3f** and **3k**. In light of these data, compound **3j** ("squarunkin A") was chosen for further evaluation as it offers the best compromise between low nanomolar activity, good membrane permeability, and sufficient kinetic solubility.

All attempts to crystallize UNC119 in complex with an inhibitor met with failure. Therefore, an exhaustive in silico analysis including docking and molecular dynamics (MD) simulations was performed to gain insight into the putative binding mode of the compounds. A visual inspection of the obtained docking-based binding modes led to a hypothetic common binding mode for nearly all compounds that is in accordance with the structure–activity relationship (see Figure 2A for the binding of squarunkin A). Owing to the size of the binding pocket and the high number of possible interactions, MD simulations were performed to strengthen this binding hypothesis. The simulation confirmed the proposed binding mode, and during the simulations, two hydrogen bonds between Glu163 as a hydrogen-bond acceptor and the two nitrogen atoms bordering the C2 alkyl linker in the molecule were identified as the most prominent interactions (Figure 2B).

Based on this binding mode, squarunkin A appears to give rise to π–π stacking interactions of the phenyl moiety with Phe196, hydrogen bonds to Asn230 and Tyr234, and additional hydrogen bonds to Glu163 and Ser218. The trifluoromethyl-substituted aryl ring is located in a hydrophobic pocket formed by Tyr236, Leu199, Leu138, Met207, and Phe196 (Figure 2A). During the MD simulations, the aryl substituent rearranges in an adjacent hydrophobic subpocket formed by aromatic (Phe196, Tyr194, Phe91) and aliphatic residues (Ile93, Val143; Figure 2B). The ethyl group of the ester substituent occupies a hydrophobic region lined by Ile105 and Val129. The latter hydrophobic contacts seem to be important for binding as compounds **3b** and **3c**, which lack the ethyl group, show no binding compared to squarunkin A (Figure S2).

Table 1: Synthesis and evaluation of squaramide-based inhibitors of the interaction between UNC119A and myristoylated cargo.[a]

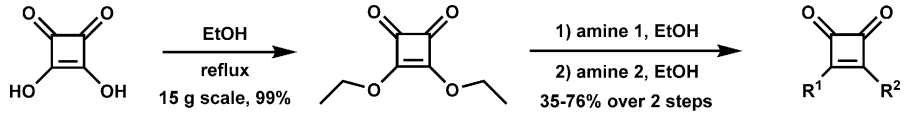

1 2 3

Compound	R^1	R^2	IC_{50} [nM]	Kinetic solubility [μM]	PAMPA [% flux]
3a	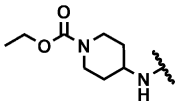	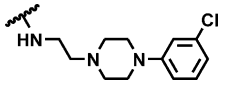	14 ± 1	20.1	51.3
3b	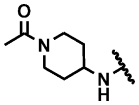	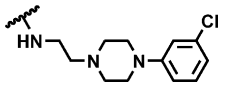	inactive	n.d.	n.d.
3c	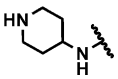	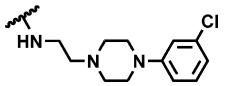	inactive	n.d.	n.d.
3d	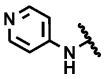	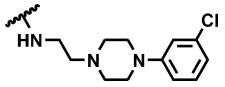	inactive	n.d.	n.d.
3e	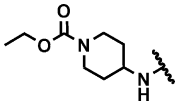	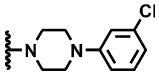	inactive	n.d.	n.d.
3f	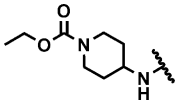	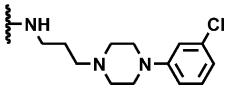	7 ± 1	269.2	22.5
3g	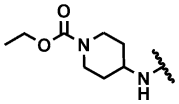	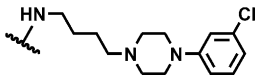	31 ± 4	n.d.	n.d.
3h	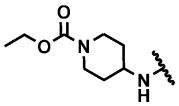	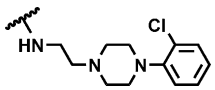	91 ± 10	n.d.	n.d.
3i	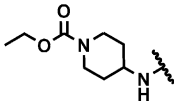	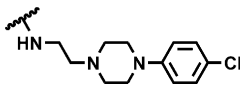	25 ± 1	n.d.	n.d.
3j	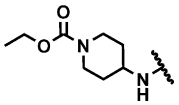	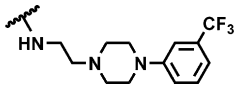	10 ± 1	19.5	48.4
3k	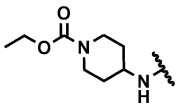	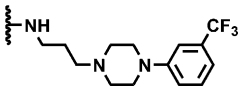	8 ± 1	23.0	30.9

[a] All data are shown as mean ± SD of three independent experiments. n.d. = not determined.

To determine the selectivity for binding to the UNC119A protein, squarunkin A was tested for the inhibition of cargo binding by other lipid-binding proteins, in particular the farnesyl-binding proteins PDE6δ,[19] AIPL1,[20] and calmodulin[21] and the geranylgeranyl-binding protein RhoGDI[22] (Figure 3). To this end, binding of fluorescently labeled myristoylated Src,[18] farnesylated Rheb,[23] and geranylgeranylated Rab1[18] peptides to the corresponding lipid-binding protein was monitored in fluorescence polarization assays. The assays revealed that only the binding of the Src peptide to UNC119A was outcompeted by squarunkin A.

For proof of target engagement by squarunkin A in a complex cellular environment, a cellular thermal shift assay (CETSA) experiment in Jurkat cell lysate using tandem MS/MS analysis readout was performed. In this experiment, the thermal stabilization of the UNC119 proteins upon binding to the ligand was determined (Figure 4A). Squarunkin A stabilizes both isoforms UNC119A and UNC119B with thermal shifts of 6.16 °C and 8.07 °C, respectively.

To determine the activity of squarunkin A in cells, its influence on the activation of Src was monitored. Myristoylation and membrane localization of Src are critical for its

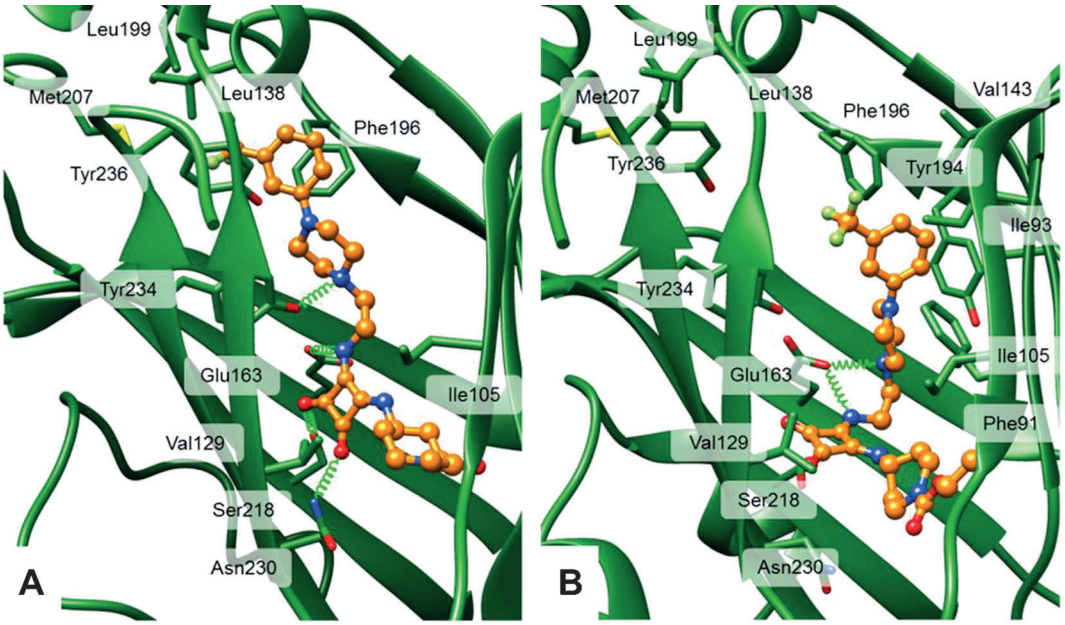

Figure 2. A) Docking- and B) molecular-dynamics-based putative binding modes of compound **3j** to UNC119A. The compound (orange, ball-and-stick representation) mainly interacts with the protein via various hydrogen bonds (green springs) while the aryl moiety occupies the hydrophobic pocket at the bottom of the binding site.

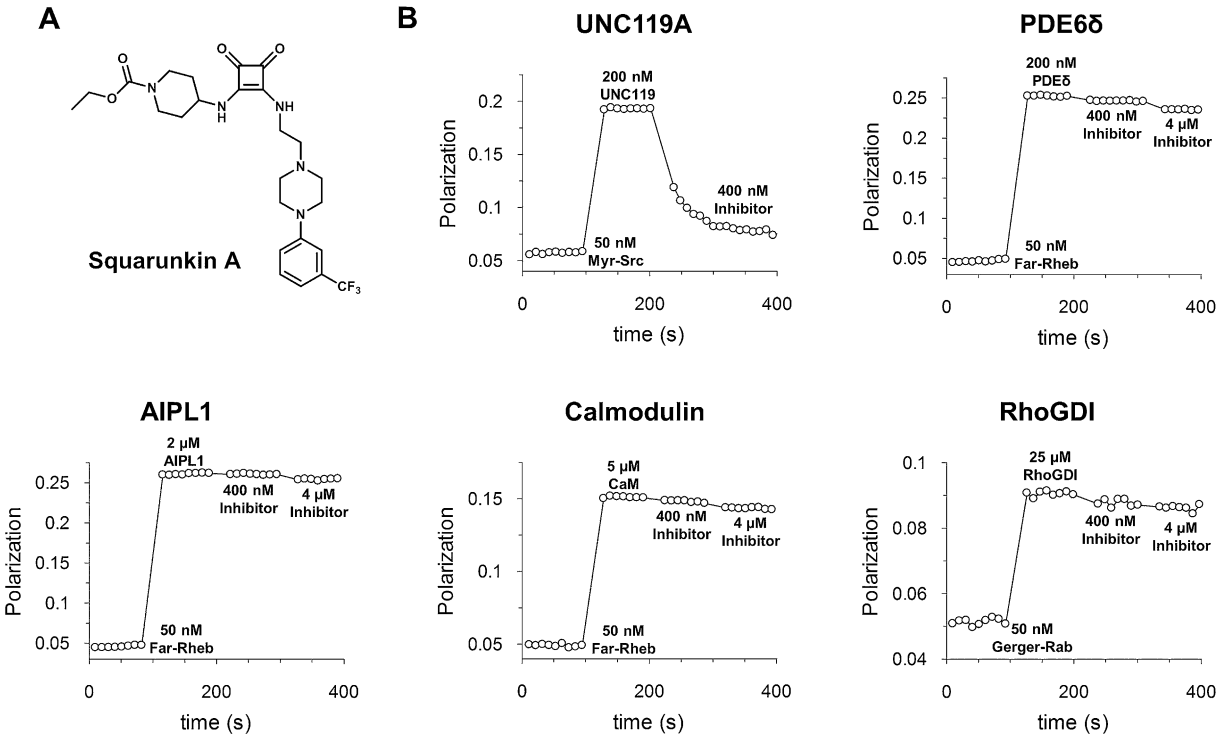

Figure 3. A) Structure of squarunkin A. B) Determination of the selective binding of squarunkin A to UNC119A compared to the lipid-binding proteins PDE6δ, AIPL1, calmodulin, and RhoGDI, as determined by means of fluorescence polarization measurements. The concentrations of the components are indicated.

kinase activity.[24] Inactive Src is phosphorylated at the regulatory tyrosine Y527 while phosphorylation of tyrosine Y416 is required for activity. Upon membrane localization, Y527 is dephosphorylated, resulting in a conformational change of Src, and Y416 is phosphorylated, yielding active Src kinase. The impact of inhibiting the UNC119–Src interaction on changes in Y416 phosphorylation of Src (and thereby its activation) was monitored by means of an in-cell Western assay[25] in the triple-negative breast cancer cell line MDA-MB-231, which expresses high levels of Src. Treatment of the

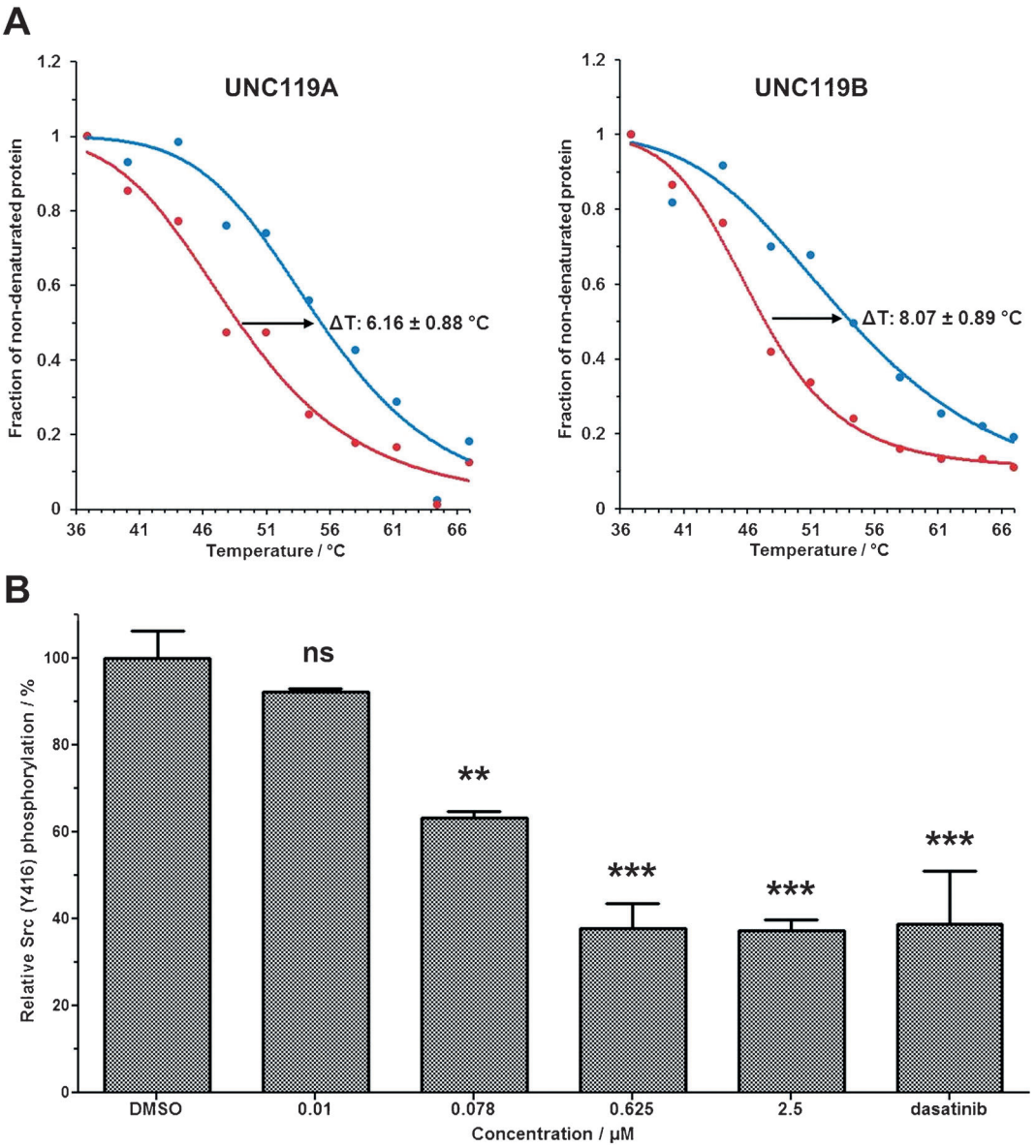

Figure 4. Biochemical evaluation of squarunkin A. A) Cellular thermal shift assay of UNC119 proteins upon treatment with DMSO control (red) and squarunkin A (blue). Lysates from Jurkat cells were treated with squarunkin A at 1 μM concentration, and thermal stabilization of the proteins was identified and quantified by means of tandem MS/MS analysis. B) Squarunkin A inhibits the phosphorylation of Y416 in Src. MDA-MB-231 cells were treated with various concentrations of squarunkin A (2.5, 0.625, 0.078, and 0.01 μM) or DMSO and dasatinib (0.078 μM) as controls. Phosphorylation of Src Y416 was detected and quantified by means of an in-cell Western assay. Data are presented as mean values ± SD ($N=4$, $n=3$) and were normalized to the amount of total Src; ns = non-significant, ** $p<0.01$, *** $p<0.001$ as determined by an unpaired, two-tailed Student's t-test.

cells with increasing concentrations of squarunkin A led to a concentration-dependent reduction of Src phosphorylation (Figure 4B). A significant decrease in phosphorylation level was observed already upon treatment with 0.078 μM of squarunkin A. At a concentration of 0.625 μM, the phosphorylation of Src (Y416) was reduced to 40%. At these concentrations and up to 10 μM, squarunkin A is non-toxic to cells and does not induce apoptosis (Figures S3 and S4). Similar results were obtained by immunoblotting (Figure S5).

In conclusion, we have developed squarunkin A as the first specific small-molecule inhibitor of the interaction between UNC119 proteins and myristoylated cargo. Molecular modeling studies suggest that squarunkin A interacts with the hydrophobic pocket of the UNC119 proteins and potently competes with lipidated cargo for binding. Squarunkin A binds to UNC119 in cell lysate and interferes with the activation of Src kinase. While mechanistic conclusions cannot be drawn from our experiments, the results demonstrate the potential of squarunkin A as a novel compound to investigate the biology of the UNC119 proteins and their myristoylated cargo proteins.

Acknowledgements

This research was supported by the Deutsche Forschungsgemeinschaft (Sonderforschungsbereich SFB 642 to A.W. and H.W.). T.M. acknowledges the Alexander von Humboldt Foundation for a Research Scholarship. C.E. is funded by a Kekulé Mobility Fellowship from the Chemical Industry Fund (FCI). O.K. thanks the German Federal Ministry for Education and Research (BMBF, Medizinische Chemie in Dortmund, Grant BMBF 1316053) for funding. We thank Christine Nowak for the cloning and expression of UNC119 protein and Dr. Petra Janning, Dr. Marc Schürmann, Jens Warmers, and Malte Metz for assistance with the establishment and analysis of CETSA experiments.

Conflict of interest

The authors declare no conflict of interest.

Keywords: chemical biology · medicinal chemistry · Src kinase · structure–activity relationships · UNC119 protein

[1] R. Constantine, H. Zhang, C. D. Gerstner, J. M. Frederick, W. Baehr, *Vision Res.* **2012**, *75*, 26 – 32, and references therein.
[2] K. J. Wright, L. M. Baye, A. Olivier-Mason, S. Mukhopadhyay, L. Sang, M. Kwong, W. Wang, P. R. Pretorius, V. C. Sheffield, P. Sengupta, D. C. Slusarski, P. K. Jackson, *Genes Dev.* **2011**, *25*, 2347 – 2360.
[3] a) H. Zhang, R. Constantine, S. Vorobiev, Y. Chen, J. Seetharaman, Y. J. Huang, R. Xiao, G. T. Montelione, C. D. Gerstner, M. W. Davis, G. Inana, F. G. Whitby, E. M. Jorgensen, C. P. Hill, L. Tong, W. Baehr, *Nat. Neurosci.* **2011**, *14*, 874 – 880; b) K. N. Gopalakrishna, K. Doddapuneni, K. K. Boyd, I. Masuho, K. A. Martemyanov, N. O. Artemyev, *J. Biol. Chem.* **2011**, *286*, 28954 – 28962; c) M. Jaiswal, E. K. Fansa, S. K. Kösling, T. Mejuch, H. Waldmann, A. Wittinghofer, *J. Biol. Chem.* **2016**, *291*, 20766 – 20778.
[4] a) O. Cen, M. M. Gorska, S. J. Stafford, S. Sur, R. Alam, *J. Biol. Chem.* **2003**, *278*, 8837 – 8845; b) M. M. Gorska, S. J. Stafford, O. Cen, S. Sur, R. Alam, *J. Exp. Med.* **2004**, *199*, 369; c) R. Vepachedu, M. M. Gorska, N. Singhania, G. P. Cosgrove, K. K. Brown, R. Alam, *J. Immunol.* **2007**, *179*, 682 – 690; d) M. M. Gorska, Q. Liang, Z. Karim, R. Alam, *J. Immunol.* **2009**, *183*, 1675 – 1684.
[5] A. D. Konitsiotis, L. Roßmannek, A. Stanoev, M. Schmick, P. I. H. Bastiaens, *Nat. Commun.*, in press.
[6] S. Zhang, D. Yu, *Trends Pharmacol. Sci.* **2012**, *33*, 122 – 128.
[7] M. D. Resh, *Nat. Chem. Biol.* **2006**, *2*, 584 – 590.
[8] a) S. A. Ismail, Y.-X. Chen, A. Rusinova, A. Chandra, M. Bierbaum, L. Gremer, G. Triola, H. Waldmann, P. I. H. Bastiaens, A. Wittinghofer, *Nat. Chem. Biol.* **2011**, *7*, 942 – 949; b) A. Chandra, H. E. Grecco, V. Pisupati, D. Perera, L. Cassidy, F. Skoulidis, S. A. Ismail, C. Hedberg, M. Hanzal-Bayer, A. R. Venkitaraman, A. Wittinghofer, P. I. H. Bastiaens, *Nat. Cell Biol.* **2012**, *14*, 148 – 158.
[9] M. Schmick, N. Vartak, B. Papke, M. Kovacevic, D. C. Truxius, L. Rossmannek, P. I. H. Bastiaens, *Cell* **2014**, *157*, 459 – 471.
[10] a) G. Zimmermann, B. Papke, S. Ismail, N. Vartak, A. Chandra, M. Hoffmann, S. A. Hahn, G. Triola, A. Wittinghofer, P. I. Bastiaens, H. Waldmann, *Nature* **2013**, *497*, 638 – 642; b) B. Papke, S. Murarka, H. A. Vogel, P. Martín-Gago, M. Kovacevic, D. C. Truxius, E. K. Fansa, S. Ismail, G. Zimmermann, K. Heinelt, C. Schultz-Fademrecht, A. Al Saabi, M. Baumann, P. Nussbaumer, A. Wittinghofer, H. Waldmann, P. I. H. Bastiaens, *Nat. Commun.* **2016**, *7*, 11360; c) G. Zimmermann, C. Schultz-Fademrecht, P. Küchler, S. Murarka, S. Ismail, G. Triola, P. Nussbaumer, A. Wittinghofer, H. Waldmann, *J. Med. Chem.* **2014**, *57*, 5435 – 5448.
[11] S. J. Parsons, J. T. Parsons, *Oncogene* **2004**, *23*, 7906 – 7909.
[12] T. J. Yeatman, *Nat. Rev. Cancer* **2004**, *4*, 470 – 480.
[13] L. C. Kim, L. Song, E. B. Haura, *Nat. Rev. Clin. Oncol.* **2009**, *6*, 587 – 595.
[14] a) Z. A. Knight, K. M. Shokat, *Chem. Biol.* **2005**, *12*, 621 – 637; b) M. E. Breen, M. B. Soellner, *ACS Chem. Biol.* **2015**, *10*, 175 – 189.
[15] a) Z. Fang, C. Grütter, D. Rauh, *ACS Chem. Biol.* **2013**, *8*, 58 – 70; b) P. Wu, M. H. Clausen, T. E. Nielsen, *Pharmacol. Ther.* **2015**, *156*, 59 – 68.
[16] A. Volkamer, D. Kuhn, F. Rippmann, M. Rarey, *Bioinformatics* **2012**, *28*, 2074 – 2075.
[17] F. Degorce, A. Card, S. Soh, E. Trinquet, G. P. Knapik, B. Xie, *Curr. Chem. Genomics* **2009**, *3*, 22 – 32.
[18] T. Mejuch, H. van Hattum, G. Triola, M. Jaiswal, H. Waldmann, *ChemBioChem* **2015**, *16*, 2460 – 2465.
[19] H. Zhang, X.-h. Liu, K. Zhang, C.-K. Chen, J. M. Frederick, G. D. Prestwich, W. Baehr, *J. Biol. Chem.* **2004**, *279*, 407 – 413.
[20] A. Majumder, K. N. Gopalakrishna, P. Cheguru, L. Gakhar, N. O. Artemyev, *J. Biol. Chem.* **2013**, *288*, 21320 – 21328.
[21] B. Sperlich, S. Kapoor, H. Waldmann, R. Winter, K. Weise, *Biophys. J.* **2016**, *111*, 113 – 122.
[22] N. H. Keep, M. Barnes, I. Barsukov, R. Badii, L.-Y. Lian, A. W. Segal, P. C. E. Moody, G. C. K. Roberts, *Structure* **1997**, *5*, 623 – 633.
[23] Y.-X. Chen, S. Koch, K. Uhlenbrock, K. Weise, D. Das, L. Gremer, L. Brunsveld, A. Wittinghofer, R. Winter, G. Triola, H. Waldmann, *Angew. Chem. Int. Ed.* **2010**, *49*, 6090 – 6095; *Angew. Chem.* **2010**, *122*, 6226 – 6231.
[24] P. Patwardhan, M. D. Resh, *Mol. Cell. Biol.* **2010**, *30*, 4094 – 4107.
[25] E. M. Egorina, M. A. Sovershaev, B. Østerud, *J. Thromb. Haemostasis* **2006**, *4*, 614 – 620.

Manuscript received: February 21, 2017
Revised: March 30, 2017
Final Article published: ■■ ■■, ■■■■

Communications

Medicinal Chemistry

T. Mejuch, G. Garivet, W. Hofer, N. Kaiser, E. K. Fansa, C. Ehrt, O. Koch, M. Baumann, S. Ziegler, A. Wittinghofer, H. Waldmann* _____ ■■■■–■■■■

Small-Molecule Inhibition of the UNC119–Cargo Interaction

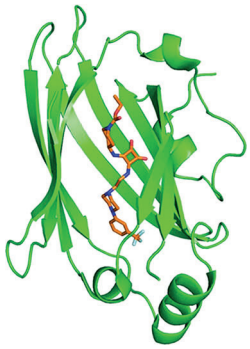

Cargo unloading: The first specific small-molecule inhibitor of the interaction between UNC119 proteins and myristoylated cargo, squarunkin A, was developed. Squarunkin A interacts with the hydrophobic pocket of the UNC119 proteins and interferes with the activation of Src kinases.